TRENDS IN SCIENCES 2025; 22(11): 10665
https://doi.org/10.48048/tis.2025.10665 RESEARCH ARTICLE

Anticancer Activity and Apoptosis Induction of Alkaloid Fraction of Kratom Leaves (*Mitragyna speciosa*) on Breast Cancer Cells: *In Vitro* and *In Silico* Studies

Puja Adi Priatna[1], Siti Rahmah[2], Retno Widyowati[3] and Sukardiman[3,*]

[1]*Doctor Program of Pharmaceutical Sciences, Faculty of Pharmacy, Airlangga University, Surabaya 60115, Indonesia*
[2]*Master Program of Pharmaceutical Sciences, Faculty of Pharmacy, Airlangga University, Surabaya 60115, Indonesia*
[3]*Department of Pharmaceutical Sciences, Faculty of Pharmacy, Airlangga University, Surabaya 60115, Indonesia*

([*]Corresponding author's e-mail: sukardiman@ff.unair.ac.id)

Received: 15 May 2025, Revised: 15 June 2025, Accepted: 25 June 2025, Published: 30 July 2025

Abstract

Breast cancer is one of the highest causes of death in women. However, cancer therapy drugs have weaknesses, low selectivity, which results in reduced efficacy. Kratom contains alkaloid group compounds that have a cytotoxic effect. This study aimed to evaluate the cytotoxic effects and apoptosis mechanisms on the alkaloid fraction of Kratom Leaves. Additionally, identify their metabolite with LC-MS/MS and molecular docking to predict its apoptotic activity. Fractionation was carried out by liquid-liquid extraction and acid-base methods. The cytotoxic test was carried out using the MTT assay method on extract and alkaloid fractions on T47D breast cancer cells. Apoptosis mechanism testing was performed using AO/EB staining. Identification of the chemical composition of alkaloid fractions with LC-MS/MS as a ligand to perform molecular docking. The proteins used as molecular docking targets are the 3ERT protein (estrogen receptor) and the 2W3L protein (Bcl-2 receptor). The alkaloid fraction of kratom leaves can provide moderate cytotoxic activity with an IC_{50} of 96.23 µg/mL against T47D cells compared to kratom leaf extract, which has weak potential with an IC_{50} value of 419.21 µg/mL. Research finds that the alkaloid fraction of kratom leaves exhibits superior cytotoxic activity in T47D cells compared to kratom leaf extract samples. The alkaloid component significantly promoted apoptotic induction compared with untreated control cells. The alkaloid fraction was found to contain 8 alkaloid compounds: 7-Hydroxymitragynine, Corynantheidine, Isorhynchophylline, Mitragynine, Pholcodine, Polyneuridinealdehyde, Rotundifolone, and Yohimbine. Moreover, polyneuridinealdehyde exhibits the greatest potential in silico against estrogen receptors, while yohimbine demonstrates significant efficacy against Bcl-2 receptors.

Keywords: Alkaloid, Apoptosis, Breast cancer, Docking, Kratom, LC-MS/MS

Introduction

Breast cancer is a disease with a high prevalence. According to GLOBOCAN (Global Burden of Cancer) data, in 2020 new cases due to breast cancer are the first order in the world, namely 2,261,419 cases (11.7%) [1]. Cancer treatment may involve chemotherapy, immunotherapy, targeted therapy, and radiation therapy [2]. Nonetheless, there are disadvantages associated with existing cancer therapies. There are significant severe side effects, and there is no cure. One cancer treatment, chemotherapy, destroys rapidly dividing cancer cells as well as rapidly dividing good cells, like those that line the mouth and intestines and those that cause hair to develop. Other adverse effects include nausea, vomiting, diarrhea, alopecia, neuropathy, and myalgia, along with the development of Multi-Drug Resistance (MDR) [3,4]. Therefore, active and selective chemicals are needed as an alternative anticancer treatment to reduce side effects and improve the comfort and quality of life of cancer patients.

Herbal therapy has been widely promoted and studied as an alternative to cancer treatment. Over 60% of clinically utilized chemotherapeutic drugs are derived from herbs, including vincristine, vinblastine, paclitaxel, and topotecan [5]. Natural anticancer chemicals often originate from the alkaloid Harvey [6] and steroid classes [7]. Alkaloids are among the most significant active ingredients found in natural herbs, and several of these substances have already been successfully developed into medications used to treat cancer. One of the plants is recognized for its cytotoxic impact and contains alkaloids, specifically kratom leaf (*Mitragyna speciosa*) [8].

Kratom leaves are commonly located in Southeast Asia. Kratom is a plant recognised for its high alkaloid content. Over 54 alkaloid chemicals have been identified in the plant, with mitragynine being one of the most dominant. Kratom contains alkaloid compounds with an indole alkaloid structure that have a significant anticancer potential. The structure of indole alkaloids similar to that the of the alkaloid compounds found in vincristine and vinblastine, which are utilised clinically as cancer therapeutics [9]. Saidin and Gooderham initially reported research on the anticancer properties of methanol extract and mitragynine components from kratom leaves, in MCL-5 lymphoblastoid cells and SH-SY5Y nerve cells [10]. Phytochemicals and their derivatives have the potential to enhance cancer treatments' efficacy while decreasing side effects. Doxorubicin and an alkaloid extract from kratom leaf were found to enhance the drug's sensitivity in A549 lung cancer cells by 2.6 to 3.4 times, suggesting that the 2 substances could work together to decrease the dosage of doxorubicin [11].

Phytochemical compounds exhibit anticancer properties by modulating the immune system, decreasing cellular proliferation, obstructing topoisomerase enzymes, and inducing apoptosis. In chemotherapy, the majority of medicines operate through an apoptosis inducing mechanism [12]. Compounds in the alkaloid category have been shown to trigger apoptosis by suppressing the production of antiapoptotic proteins (Bcl-2, Bcl-xL, Mcl-1) and enhancing the activity of apoptosis execution receptors (caspase-3) [13].

This research investigated the activity and mechanism of the alkaloidal fraction derived from kratom leaves. Previous research has assessed the cytotoxic effects of kratom plant alkaloids on colon, leukemia, nasopharyngeal, nerve, and lung cancer cells *in vitro* [11,14-16]. Nonetheless, there are no definitive findings on the activity and mechanism of apoptosis induction by kratom leaf alkaloid fractions in breast cancer.

Techniques for detecting apoptosis induction have been established by morphological alterations and cell surface markers *in vitro*. A method for detecting apoptosis involves acridine orange (AO) / ethidium bromide (EB) double labeling observed with a fluorescence microscope. AO/EB can reveal alterations in the cell membrane during apoptosis [17]. Molecular docking is an efficient technique for identifying bioactive compounds and elucidating their binding mechanisms and interactions with protein targets [18]. The chemical composition of plants can be determined using a liquid chromatography-mass spectrophotometry / mass spectrophotometry (LC-MS/MS) instrument [19]. A combined approach of in silico methodologies and chromatography / spectroscopic analyses can be employed to ascertain bioactive compounds present in extracts or fractions [20,21].

This study aimed to assess the cytotoxic effects and apoptosis mechanisms of AO/EB on the alkaloid fraction derived from kratom leaves in breast cancer cells *in vitro*. Additionally, this study used LC-MS/MS to identify the metabolite composition of the alkaloid fraction of kratom leaves and in silico molecular docking to predict its apoptotic activity.

Materials and methods

Instruments

The tools for the extraction and fractionation process include a rotary evaporator (Buchi), chromatography vessel, and 254 and 366 nm UV lamps. The tools for cytotoxicity and apoptosis tests include a CO_2 incubator (New Brunswick, Galaxy 170R), centrifuge (Hermle Siemensstr-25D-78564), sonicator, LAF (Mascotte LH-s), micropipette (Socorex), 96-well plate (Biologix®), 60 mm culture dish (Nest), microplate reader (Biochrom Asys UVM 340), and fluorescence microscope inverted Nikon eclipse Ts2R at a magnification of 100×. Analysis for chemical compound content by Ultra Performance Liquid Chromatography (UPLC), C18 (1.8 µm 2.1×100 mm)

HSS (Waters), and the MassLynx V4.1 SCN884 (Waters Inc.) Tools for molecular docking, namely a ASUS X409FJ computer, including an Intel® Core™ i5 8265U processor operating at 1.80 GHz and equipped with 4 GB of Random Access Memory (RAM), ChemDraw 20.0 programme, Chem3D 20.0, AutoDockVina in the PyRx 0.8 system, AutoDockTools 4.2.6, and Discovery Studio Visualizer v.19.1.0.18287.

Materials

The plant material in this study was kratom leaf dried plant (*Mitragyna speciosa* Korth.) from the Pontianak area, West Kalimantan, and its authenticity was identified at the UPT Herbal Materia Medica Laboratory, Batu, East Java, Indonesia with letter number No. 074/823/102.20-A/2022. The following chemicals were employed for extraction and fractionation, included ethanol, dichloromethane p.a. (Merck), distilled water, ethanol p.a. (Merck), n-hexane p.a. (Merck), ammonium formic p.a (Merck), acetonitrile p.a (Merck), and formic acid p.a (Merck). Silica gel 60 PF254 (aluminium sheets) (Merck: 1.05554.0001) was employed for thin layer chromatography.

Materials for *in vitro* apoptosis induction and activity tests, namely RPMI-1640 medium (Sigma-Aldrich), Fetal Bovine Serum F2442 (Sigma-Aldrich) essential nutrients and growth factors, penicillin-streptomycin P4333 (Sigma-Aldrich), amphotericin B A2942 (Sigma-Aldrich), Phosphate Buffer Saline (PBS) 10010031 pH 7.4 (Gibco™), DMSO 472301 (Sigma-Aldrich), MTT (3-(4,5-dimethylthiazol-2-yl)-2,5-diphenyltetrazolium bromide) Cell Count Kit 23506-80 (Nacalai Tesque), SDS L3771 (sodium dodecyl sulphate) stopper in 0.01 N HCl (Sigma-Aldrich), Acridine Orange A6014 hemi(zinc chloride) salt for nucleic acid staining (Sigma-Aldrich), ethidium bromide E1510 for nucleic acid stain (Sigma-Aldrich).

Extraction and fractionation of kratom leaf alkaloids

The maceration method was used to extract the powder from Kratom leaf dried plant for 24 h using 2.5 L of 96% ethanol twice. We gathered and evaporated all of the filtrate. Following the drying process, the concentrated extract's yield percentage was computed. The fractionation procedure was also conducted using Sharma *et al.* [22] methodology. The kratom leaf dry extract was redissolved in 96% ethanol and then acidified with 10% HCl to achieve a pH of 2 - 3. The liquid-liquid extraction process was carried out using n-hexane with a ratio of 1:1. After the N-hexane phase was extracted, the water phase was separated and fractionated by alkalinization using 10% Na_2CO_3 until it reached pH 8 - 9. After that, the water fraction was subjected to liquid-liquid extraction using dichloromethane with a ratio of 1:1. The water phase and dichloromethane phase were separated and collected. The extract samples, n-hexane fractions, and dichloromethane fractions were identified for chromatogram patterns using silica gel F254 TLC plates. The mobile phase used was n-hexane:ethyl acetate (3:7). The chromatogram pattern was identified under visible light, under UV 366 nm, under UV 254 nm, and sprayed with Dragendorff's reagent.

Cell culture

The *In Vitro* Laboratory Research Center 1 collection of Airlangga University's Faculty of Pharmacy provided the T47D breast cancer cells. The first step in cell preparation is to use a microscope to check the stem cell culture's cells in a dish for readiness. Cell harvesting was at its best when 70% - 80% of the cells were confluent. RPMI, which contained 10% FBS, 1% Fungizole, and 1% Pen-Strep, was the growth medium utilized.

Cytotoxic activity test

Cytotoxicity was evaluated using the MTT assay, which started with the preparation of a sample solution in 7 different concentrations by gradual dilution with media. The samples tested consisted of extract, n-hexane fraction, and dichloromethane fraction from kratom leaves. The dichloromethane fraction obtained was defined as the alkaloid fraction. The sample is solubilized with DMSO. Cancer cells were counted and diluted, with up to 100 µl of cells transferred into the wells at a concentration of 5×10^3 cells per well. Four empty wells were designated for media blanks. Cells had incubation for a duration of 24 h. Ethanol extracts were prepared at various concentrations: 200, 250, 300, 350, 400, 450 and 500 µg/mL. n-Hexane fraction were prepared at various concentrations: 50, 75, 100, 200, 300, 400 and 500 µg/mL. Alkaloid fraction were

prepared at various concentrations: 50, 75, 100, 125, 150 and 175 µg/mL. Doxorubicin were prepared at various concentrations: 0.05, 0.1, 0.2, 0.3, 0.4, 0.5 and 0.6 µg/mL. The sample concentration series was then transferred into the wells and incubated for 24 h. At the conclusion of the incubation period, 100 µl of MTT reagent was introduced to each well, including the control media devoid of cells. Incubate cells for 2 to 4 h in a CO_2 incubator. The cells' condition was assessed using an inverted microscope. Upon clear formation of formazan, 100 µl of 10% SDS in 0.01 N HCl is added to the stopper. Wrapped the well plate in paper or aluminum foil and incubate in a dark environment at room temperature for one night. The absorbance was measured using an ELISA reader at a wavelength of 550 - 600 nm, specifically at 570 nm.

Apoptotic induction double staining test

Confluent T47D cell cultures were harvested and counted. The apoptosis assay utilizing the AO/EB double staining method employed 5×10^4 cells each well, with an amount of 200 µl each well. The cell suspension was uniformly applied to the coverslip and subsequently incubated for a duration of 3 to 30 min to facilitate cell adhesion to the coverslip. Add 800 µL of media to the well gradually and incubate for 36 h in a CO_2 incubator. The treatment of T47D cells involved a control treatment and the active alkaloid fraction sample at its IC_{50} concentration, followed by a 24 h incubation period. The culture media was discarded, and the cells were washed with PBS. The cover slip containing the cells was then placed on a glass object and treated with 10 µL of acridine orange/ethidium bromide (AO/EB) mixture reagent. Cell morphology was observed using a fluorescence microscope [23]. The calculation of cells that experience apoptosis, necrosis, and living cells was carried out in 3 replications with the results of the average percentage of the cell population ± SD. Each replication was calculated at least 200 total cells expressing apoptosis, necrosis and living cells in each sample. The percentage data of apoptosis, necrosis, and live cells from each sample were then statistically tested.

Detection of chemical content with LC-MS/MS QTOF

The Ultra Performance Liquid Chromatography (UPLC) System was used, with Column C18 (1.8 µm; 2.1×100 mm) HSS and temperatures of 50 °C for the column and 25 °C for the room. A mobile phase comprising Water + 5 mmol Ammonium Formate (phase A) and Acetonitrile + 0.05% Formic Acid (phase B) was utilized with a gradient method: 0 min, 95:5 (A:B); 2 min, 75:25 (A:B); 3 min, 75:25 (A:B); 14 min, 0:100 (A:B); 15 min, 0:100 (A:B); 19 min, 95:5 (A:B); 23 min, 95:5 (A:B), with a flow rate of 0.2 mL/min. ESI charge, mass range of 50 - 1200 m/z in positive mode. Additionally, the effective energy spans from 4 to 60 electron volts, with a desolvation gas flow of 793 l/h and a cone gas flow of 0 l/h. Furthermore, the ions produced by the detector were separated using the Q-ToF analyzer. The Masslynk V4.1 application was utilized for data collecting and processing to assess the chromatogram peaks. A search of books and internet databases was performed to ascertain the m/z value for a particular molecular ion. The selection criteria for identified compounds are determined by the degree to which the compounds analyzed via LC-MS/MS correspond to those listed on the library website or in other scholarly works, specifically regarding their chemical formula, m/z, and fragmentation patterns. The library employs the online database located at https://hmdb.ca/

Preparation ligan and protein

This study collected compound data from the LC-MS/MS results of kratom leaf alkaloid fractions. Every compound to be tested was looked up using SMILES on the PubChem website (https://pubchem.ncbi.nlm.nih.gov/). A 2-dimensional structure was made using MarvinSketch in *mol format, and its 3-dimensional structure was made using VegaZZ in *pdb format and PyRx 0.8 in *pdbqt format.

Molecular docking analysis was conducted to investigate the binding mode of compounds within the active site of the ligand-binding domain of human estrogen receptor α in complex with 4-hydroxytamoxifen (PDB: 3ERT) and Bcl2-xL Phenyl Tetrahydroisoquinoline Amide Complex (PDB: 2W3L). The native ligand of 3ERT is 4-hydroxytamoxifen, while the native ligand of 2W3L is 1-(2-{[(3S)-3-(aminomethyl)-3,4-dihydroisoquinolin-2(1H)-yl]carbonyl}phenyl)-4-chloro-5-methyl-N,N-diphenyl-1H-pyrazole-3-carboxamide. The protein structures of 3ERT and 2W3L were generated utilizing AutoDock

Tools. All atypical residues and water molecules were eliminated from the foundational structure. Additionally, the system was enhanced by incorporating all absent hydrogen atoms and Kollman charges. The synthesized protein receptors were subsequently exported in pdbqt format and directly positioned into the PyRx workspace directory.

Docking molecular

The prepared macromolecules receive preliminary assessments and method validation to confirm the validity of the molecular docking procedure for the test ligand. Validation of the docking method for the ligand was conducted to ascertain the conformation of the native ligand. This involves the formation of a grid box from the native ligand to identify the coordinates of the active site of the target receptor macromolecule. The docking method was validated to examine the 3D conformation of the cocrystal ligand and the copy ligand for the target protein utilizing PyMOL software, expressed as a Root Mean Square Deviation (RMSD) value ≤ 2Å. The molecular docking test was executed with 5 repetitions using identical grid box configurations.

Results and discussion

Extraction and fractionation of ethanol extract of kratom leaves

The extraction of kratom leaf dried plant was performed using the maceration method. The dried plant powder was extracted with 96% ethanol, and the procedure was repeated 3 times. The extraction of Kratom Leaf Dried plant yielded 30.29% of the initial weight of the kratom leaf dried plant powder. Fractionation of 96% ethanol extract of kratom leaves using the acid-base method and liquid-liquid extraction produced a final result of dichloromethane fraction with a yield of 18.28% of the weight of dry kratom leaf extraction results. Using the acid-base method on kratom leaf extract can increase the main alkaloid content in the plant [22].

Alkaloid content phytochemical test

The chromatogram patterns of the extract, n-hexane fraction, and dichloromethane fraction were analyzed using silica gel F254 with n-hexane:ethyl acetate (3:7) as the eluent and Dragendorff's reagent, as illustrated in **Figure 1**. The dichloromethane fraction, presumed to contain a higher concentration of alkaloids, exhibited a more intense orange hue compared to the other samples. The intensified orange complex generated upon application of Dragendorff's reagent can be utilized to identify and confirm the presence of alkaloids at a concentration range of 0.06 - 50 µg/mL [24]. Therefore, the dichloromethane fraction obtained has been defined as the alkaloid fraction.

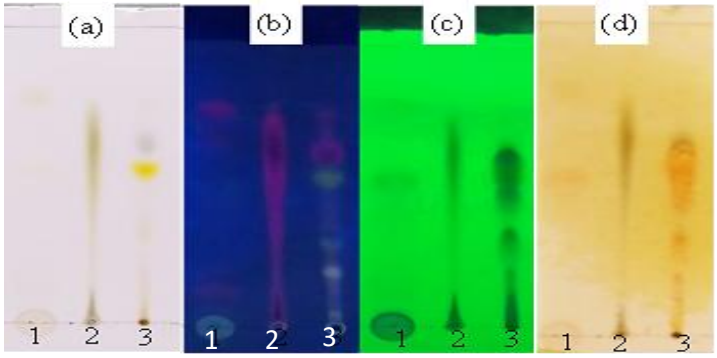

Figure 1 Alkaloid phytochemical test results using a TLC plate. 1). Extract; 2). n-hexane fraction; 3). dichloromethane fraction; (a) Before spraying reagent, b). UV 366, c). UV 254, d). Dragendroff spotting.

Cytotoxicity activity test

The MTT assay is a method performed to evaluate cytotoxicity and cell viability. Absorbance measurements of T47D cells were conducted using a Microplate Reader at a wavelength of 570 nm, with 3 replicates for each measurement. Following the use of the test compound, the viability of T47D cells was assessed using the percentage of live cells. **Figure 2** shows the percentage viability of T47D cells after they were treated with doxorubicin, extract, alkaloid, and n-hexane fraction from kratom leaves. The activity test of kratom leaf extract at a concentration of 500 µg/mL resulted in a reduction of T47D viable cells to 23.76%. The alkaloid fraction of kratom leaves at a concentration of 175 µg/mL can reduce the percentage of viable T47D cells to 1.92%. The n-hexane fraction of kratom leaves at a concentration of 500 µg/mL can reduce the percentage of viable T47D cells to 26.3%. The doxorubicin at a concentration of 0.6 µM can reduce the percentage of viable T47D cells to 6.06%. The IC_{50} of the extract was 419.21 ± 38.19 µg/mL, the IC_{50} of the alkaloid fraction was 96.23 ± 3.23 µg/mL, the IC_{50} of the n-hexane fraction was 393.51 ± 18.87 µg/mL, and the IC_{50} of doxorubicin, the positive control, was 0.14 ± 0.08 µg/mL (0,25 ± 0,14 µM).

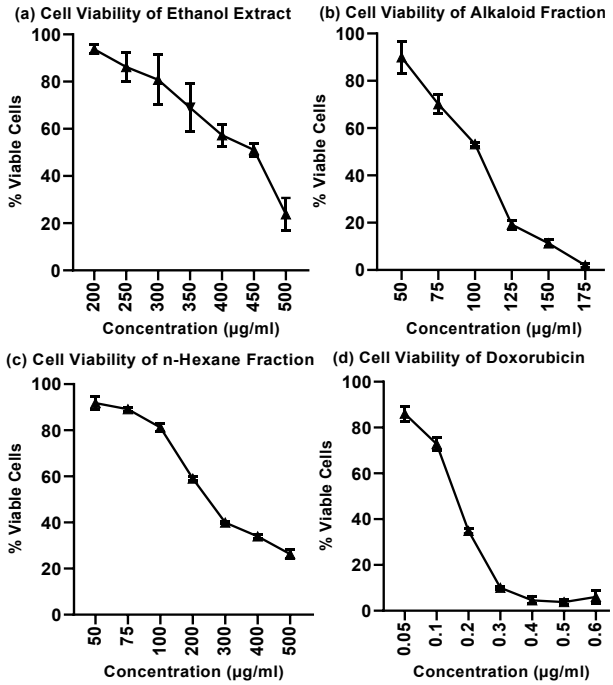

Figure 2 Graph of the percentage of T47D cell viability against treatment of (a) ethanol extract of kratom leaves, (b). alkaloid fraction of kratom leaves, (c) n-hexane fraction of kratom leaves, and (d) doxorubicin. Data represents SEM of 3 independent repeats, and each point of the graphic represents the average concentrations.

According to the reference IC_{50} value from the National Cancer Institute (NCI), strong cytotoxic effects are characterised by IC_{50} values of less than 21 µg/mL, moderate cytotoxic effects by IC_{50} values ranging from 21 to 200 µg/ml, and weak cytotoxic effects by IC_{50} values between 201 and 500 µg/mL [25]. The IC_{50} results for extract and n-hexane fraction of kratom leaf classified in the weak category, while the alkaloid fraction of kratom leaves is classified in the moderate category. This is similar to the study by Dominic *et al.* [15], which found that the alkaloid part of kratom leaves is more active than the methanol extract. The methanol extract of kratom leaves has an IC_{50} of 133.71 ± 0.72 µg/mL, whereas the alkaloid extract demonstrates an IC_{50} of 32.16 ± 0.94 µg/mL in nasopharyngeal cancer cells.

Table 1 IC_{50} value of extract, alkaloid fraction, n-hexane fraction and doxorubicin on T47D cells.

Sample	IC_{50} (µg/mL) ± SD [a]	Category Activity[c]
Kratom Leaf Extract	419.21 ± 38.19	Weak
n-Hexane Fraction of Kratom Leaves	393.51 ± 18.87	Weak
Alkaloid Fraction of Kratom Leaves	96.23 ± 3.23	Moderate
Doxorubicin[b]	0.14 ± 0.08	Strong

[a] IC_{50} in the table is represented as mean ± SD (n = 3)

[b] Positive Control

c Category activity according from the National Cancer Institute (NCI)

The results of the positive control of doxorubicin were classified inside the strong cytotoxicity category. Another study confirmed that doxorubicin exhibits significant efficacy against T47D cancer cells, as evidenced by MTT assay findings demonstrating an IC_{50} of 0.20 ± 0.02 µg/mL [26]. **Table 1** shows the IC_{50} results and activity category for samples and controls.

Induction apoptotic test result using double staining AO/EB

Based on **Figure 3**, the number of cells going through apoptosis was higher than that of normal living cells and necrotic cells. Significant differences in each cell phase apoptosis, necrosis, and living cells were caused by the treatment of kratom leaf alkaloid fractions, according to the results of ANOVA statistical data and post hoc Bonferroni with significance at $p < 0.05$. Treatment of T47D cells with alkaloid fraction significantly enhanced apoptotic induction compared to untreated control cells ($p < 0.05$). The apoptosis assay with AO/EB shown that the alkaloid fraction exhibited a cell population distribution of 79.98 ± 2.05% for apoptosis, 3.76 ± 0.54% for necrosis, and 16.36 ± 2.31% for normal cells. The control group shows cell population percentages of apoptosis, necrosis, and normal cells at 2.67 ± 0.25%, 1.33 ± 0.33%, and 96.00 ± 0.51%, respectively.

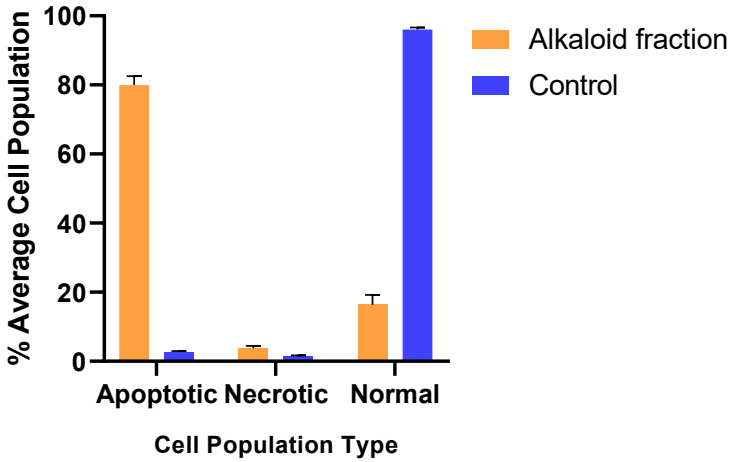

Figure 3 Graph of the percentage of viable cell population, apoptosis, and necrosis in T47D cells for the control group and treatment with kratom leaf alkaloid fraction.

Cells exhibiting red fluorescence signify necrotic cells. Cells exhibiting green fluorescence signify normal, viable cells. Normal cell groups exhibit circular nuclei uniformly positioned at the center of each cell. Fragmented cells signify apoptosis in progress. Cell groups exhibiting early apoptosis will display nuclei with yellow-green fluorescence when stained with AO, concentrated in crescents or granules on one side of the cell. Cell groups exhibiting late apoptosis will display cell nuclei with orange fluorescence when stained with ethidium bromide (EB) [17].

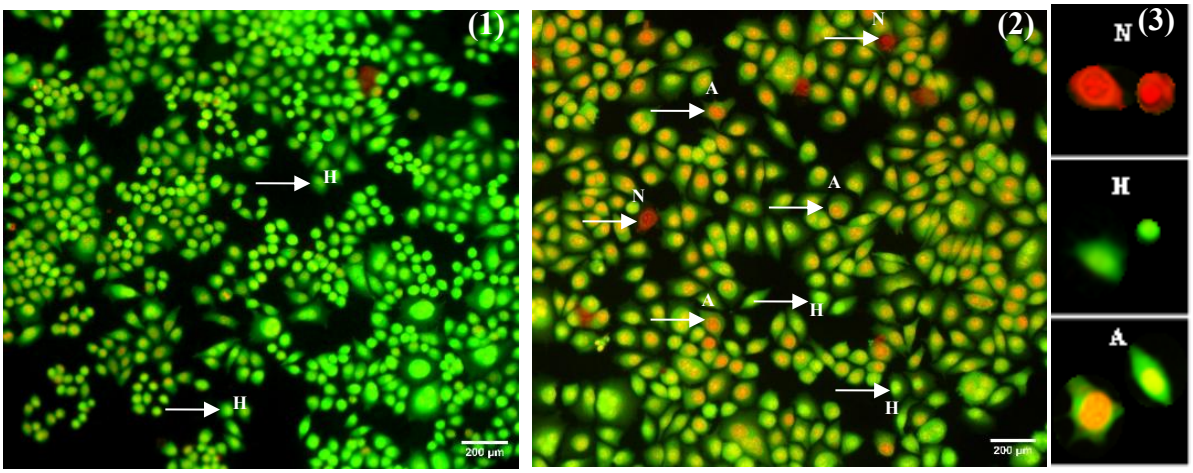

Figure 4 The results of the morphological imaging of T47D cells utilizing AO/EB staining, cells were viewed and counted using a microscope at 100× magnification and scale bar 200 µm. (1) Cells control; (2) The treatment using alkaloid fraction IC_{50} concentration; (3) Illustration of the differences between populations of cells. (→ H) Normal living cells; (→A) apoptotic cells; (→N) necrotic cells.

Based on **Figure 4**, the alkaloid fraction sample of kratom leaves exhibits an apoptotic mechanism, as evidenced by many cells with intact plasma membrane architecture that appears green, with condensed chromatin indicative of early apoptosis, and late apoptotic cells characterized by a brilliant green-orange hue. The alkaloid fraction of kratom leaves may induce apoptosis, as it is reported to contain indole alkaloid chemicals [9]. Previous research indicated that the indole alkaloids harmine from *Peganum harmala* can trigger apoptosis in MCF-7 breast cancer cells by inhibiting the Bcl-2 protein [27].

Identification of compounds contained with LC-MS/MS

Figure 5 displays the results of the chromatogram data obtained. The analysis of principal ions and molecular formulas of compounds was conducted utilizing the MassLynx V4.1 SCN884 application from Waters Inc. The outcomes of compound interpretation are presented in **Table 2**. Data interpretation showed the presence of 8 alkaloid compounds, including 7-Hydroxymitragynine at RT 6.77, Corynantheidine at RT 6.91, Isorhynchophylline at RT 6.07, Mitragynine at RT 7.08, Pholcodine at RT 8.22, and Polyneuridinealdehyde.

The majority of research on kratom leaves focuses on the primary indole alkaloid, mitragynine [9]. The alkaloid fraction sample primarily comprises mitragynine, which exhibits the highest peak percentage relative to other compounds. Mitragynine is documented to comprise up to 66% of the alkaloid fraction in kratom leaves [28].

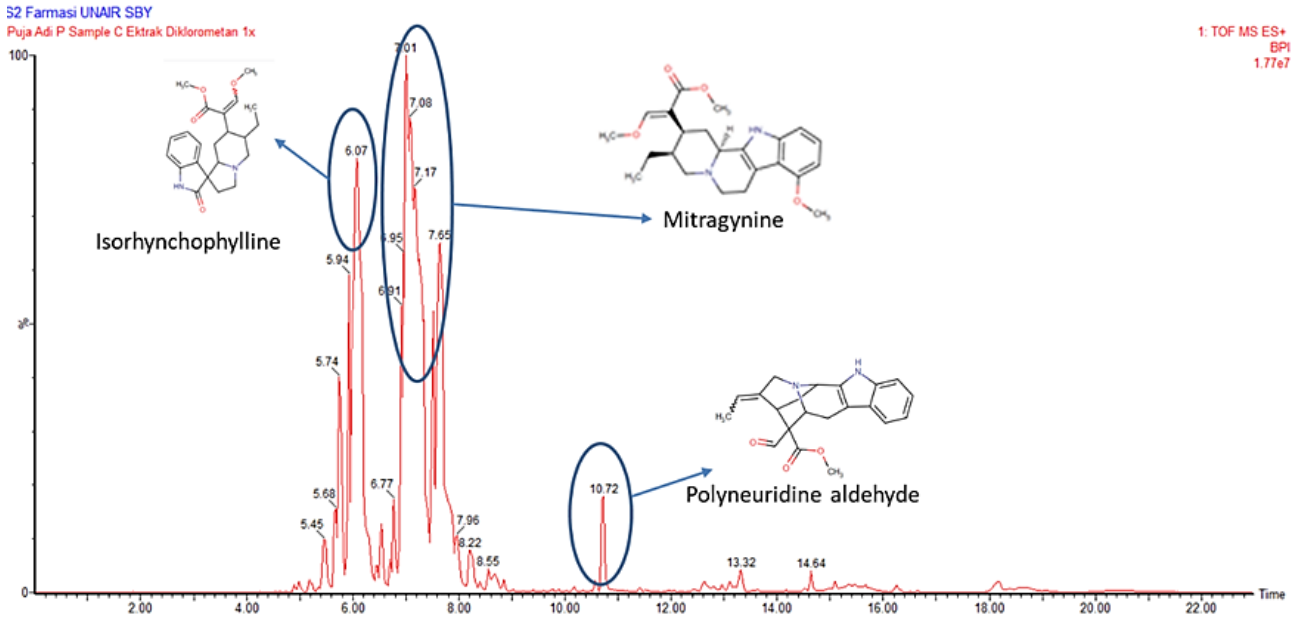

Figure 5 Chromatogram results of the alkaloid fraction of kratom leaves with the LC-MS/MS instrument LC-MS/MS identification of the compounds present in the kratom leaves' alkaloid fraction.

Table 2 Results of Analysis of Compound Identification with LC-MS/MS.

RT (min)	*Mass* m/z	*Calculated* m/z	Ion Mayor Spectra MS/MS	Molecular Formula	Identification Compound	Structure	Reference
4.97	355.2043	355.2022	330.1117 315.0883 199.0884 182.9869	$C_{21}H_{26}N_2O_3$	*Yohimbine*	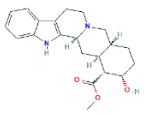	[38]
5.94	401.2086	401.2076	385.2161 369.1845 153.1891 137.0615	$C_{22}H_{28}N_2O_5$	*Rotundifoline*	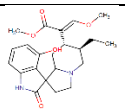	HMDB
6.07	385.2120	385.2127	353.1892 241.1361 160.0776 130.0662	$C_{22}H_{28}N_2O_4$	*Isorhynchophylline*	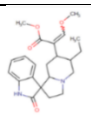	[28]
6.77	415.2237	415.2233	401.2069 321.1599 271.1442 190.0871	$C_{23}H_{30}N_2O_5$	*7-hydroxymitragynine*	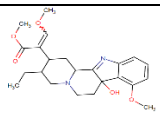	[29,38]
6.91	369.2180	369.2178	144.0811 204.0812 337.1913 328.1544	$C_{22}H_{28}N_2O_3$	*Corynantheidine*	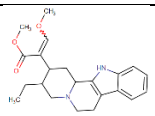	[28,38]
7.08	399.2296	399.2284	367.2023 174.0924 238.1447 351.1714	$C_{23}H_{30}N_2O_4$	*Mitragynine*	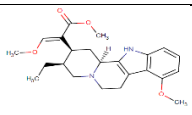	[28,38]

RT (min)	*Mass* m/z	*Calculated* m/z	Ion Mayor Spectra MS/MS	Molecular Formula	Identification Compound	Structure	Reference
8.22	399.2280	399.2284	381.1812 328.1559 174.0911 154.0652	$C_{23}H_{30}N_2O_4$	*Pholocodine*	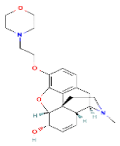	HMDB, Chemspider
10.58	351.1709	351.1709	319.1447 291.1446 261.1015 179.1431	$C_{21}H_{22}N_2O_3$	*Polyneuridine aldehyde*	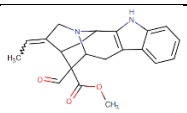	HMDB

Docking molecular

The compounds from the extract and alkaloid fractions were analyzed through molecular docking with Bcl-2 and estrogen proteins. Estrogen protein was chosen because 2 - 3 of breast cancer growth depends on estrogen. Indole alkaloids are reported to have anti-tumor and anti-estrogenic effects. Indole alkaloid derivatives from benzimidazole have potent anti-proliferative activity with an IC_{50} value of 32.2 µmol/L against MCF-7 (positive estrogen receptor) and an IC_{50} of 22.3 µmol/L against MDA-MB-231 (negative estrogen receptor) [29]. In chemotherapy treatment, most drugs have an apoptosis induction mechanism [12]. Bcl-2 protein is an antiapoptotic protein that can inhibit the apoptosis mechanism [30]. Overexpression of Bcl-2 protein is present in more than half of all cancers, regardless of cancer type [31]. The indole alkaloid compound harmine from *Peganum harmala* has been reported to induce apoptosis of MCF-7 breast cancer cells by inhibiting Bcl-2 protein [27].

Table 3 Gridbox configurations and RMSD values of macromolecular targets.

Protein	PDB ID	*Grid Center*			Grid Size	RMSD
		X	Y	Z		
Bcl-2	2W3L	28.006	38.007	5.003	25	1.641
Estrogen	3ERT	32.013	−1.874	24.312		0.915

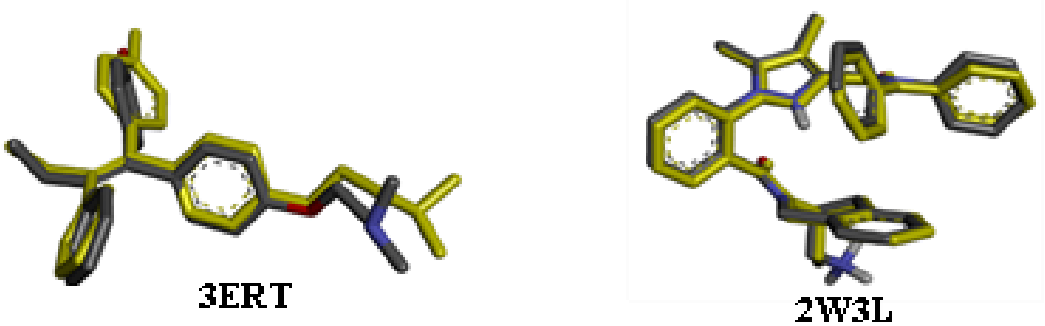

Figure 6 The overlay between native ligand crystallographic structure (yellow) and re-docking result (grey) The validation results indicate a Root Mean Square Deviation (RMSD) value of under 2 Å, confirming the validity of the docking protocol. The validation outcomes of the docking method are presented in **Table 3** and **Figure 6** with estrogen receptor (PDB: 3ERT) and Bcl2-xL Phenyl Tetrahydroisoquinoline Amide Complex (PDB: 2W3L).

Table 4 The binding free energy values (ΔG) of compounds in the alkaloid fraction.

Test ligand	$\Delta G_{binding}$ (kkal/mol)	
	Bcl-2	**Estrogen**
Native Ligand	−10	−10
Doxorubicin	−6.9	−8.7
7-Hydroxymitragynine	−6.7	−7.9
Corynantheidine	−6.7	−7.9
Isorhynchophylline	−6.9	−7.9
Mitragynine	−6.6	−8.1
Pholcodine	−7	−8.3
Polyneuridinealdehyde	−6.7	−8.3
Rotundifolone	−6.9	−7.8
Yohimbine	−8.9	−8.2

Table 5 Amino acid residues involved in interaction of ligand-protein.

Test ligand	**Amino acid residues involved in interaction of ligand-protein**	
	Bcl-2	**Estrogen**
Native Ligand	ARG105, PHE63, ALA108, LEU96, ASP70, PHE71, TYR67, MET74, VAL92, ARG88, PHE112, GLU95	GLY521, HIS524, MET528, MET421, LEU525, TRP383, ILE424, LEU428, PHE404, LEU349, LEU346, LEU391, ALA350, LEU387, GLU353, ARG394
Doxorubicin	ARG105, GLU95, LEU96, ASN102, PHE63, ALA108, TYR67, ASP99, ARG98, VAL92, PHE112, MET74	LYS531, ASP351, ALA350, LEU354, MET522, LEU525, TRP383, MET522, TYR526, ALA350, THR347, CYS530, VAL533, LEU539
7-Hydroxymitragynine	TYR67, ASN102, ARG105, LEU96, PHE71, MET74, ASP70, PHE63, ALA108, GLY104	LYS531, ALA350, TRP383, LEU354, ASP351, LEU536, PRO535, LEU346, MET343, THR347, LEU525, MET528, TYR526, LYS529
Corynantheidine	ASN102, ARG105, TYR67, LEU96, ALA108, PHE112, MET74, PHE71, PHE63	PRO535, LEU536, TYR526, TRP383, VAL534, ASP351, LEU525, LYS529, TYR537, GLU380
Isorhynchophylline	ARG105, LEU96, ALA108, TYR67, ASP70, PHE71, MET74, PHE63, PHE112, VAL92, GLY104	ASP351, LEU536, TRP383, MET522, LEU525, VAL534, PRO535, LEU354, TYR526, THR347, LYS529
Mitragynine	ARG105, ASN102, ALA108, MET74, PHE71, LEU96, PHE112, PHE6, TYR67, ASP70	ALA350, TRP383, LYS531, LEU354, ASP351, VAL534, LEU536, VAL533, PRO535, LEU346, MET343, THR347, LEU525, MET528, TYR526, LYS529
Pholcodine	ARG105, PHE71, PHE63, TYR67, LEU96, ASP99, GLU95, ALA108, VAL92, PHE112, ASP70, MET74	LEU536, TRP383, LEU384, THR347, LEU525, MET528, TYR526, LYS529, VAL534, LEU539, LEU346, ILE424, MET343, ALA350, ASP351
Polyneuridinealdehyde	ARG105, PHE63, PHE71, LEU96, ALA108, GLY104, ASN102, MET74, ASP70, TYR67	GLU353, LEU346, LEU387, TRP383, LEU525, ALA350, LEU391, THR347, ARG394, LEU349, PHE404, LEU384, GLY420, MET343, HIS524, ILE424, MET421, MET388, LEU428, GLY521

Test ligand	Amino acid residues involved in interaction of ligand-protein	
	Bcl-2	**Estrogen**
Rotundifolone	TYR67, LEU96, VAL92, PHE63, PHE112, ALA108, MET74, PHE71, ASP70	LEU525, HIS524, ILE424, MET388, LEU384, GLY521, GLY420, MET421, MET343, LEU346, THR347, ALA350, TRP383
Yohimbine	ALA108, GLU95, LEU96, VAL92, MET74, TYR67, PHE71, ASP70, PHE63, PHE112, PHE109	MET522, LYS531, LEU536, LYS529, TRP383, TYR526, MET528, LEU525

The parameter utilized to assess the affinity of ligands for receptors is the binding free energy (ΔG). A lower ΔG value suggests increased compound activity [32]. The analysis of the ΔG value from molecule docking results on the 3ERT estrogen receptor is presented in **Table 4**. The redocking of the native ligand showed a ΔG value of −10 kcal/mol, attributed to hydrophobic interactions and hydrogen bonds. Hydrogen bonds form at the Asp351 and Gly521 residues. Shiau *et al.* [33] stated that the interaction between the native ligand (4-hydroxytamoxifen) and the alpha estrogen receptor induces a conformational alteration in the 12th helix, resulting in the closure of the coactivator binding site, thereby inhibiting the signal transduction process and cell proliferation.

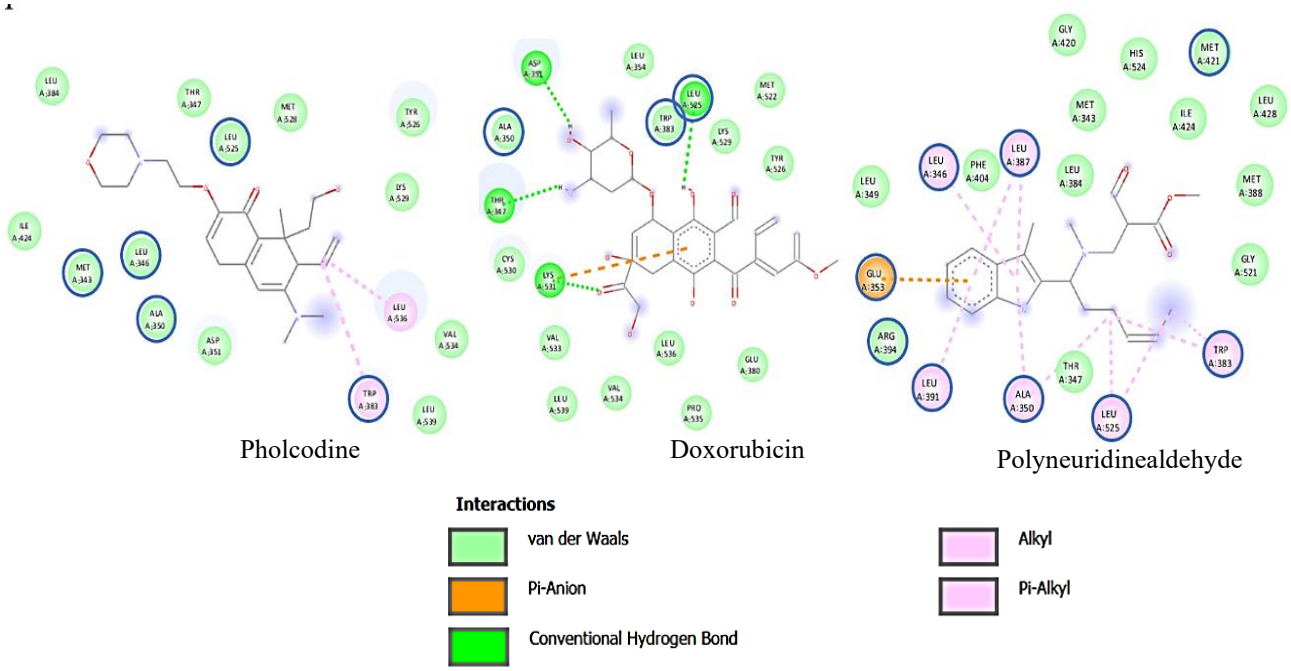

Figure 7 The interaction of Pholcodine and Polyneuridinealdehyde compounds was compared with doxorubicin on the estrogen receptor. Blue circles on amino acids indicate amino acid residues that are similar to the native ligand.

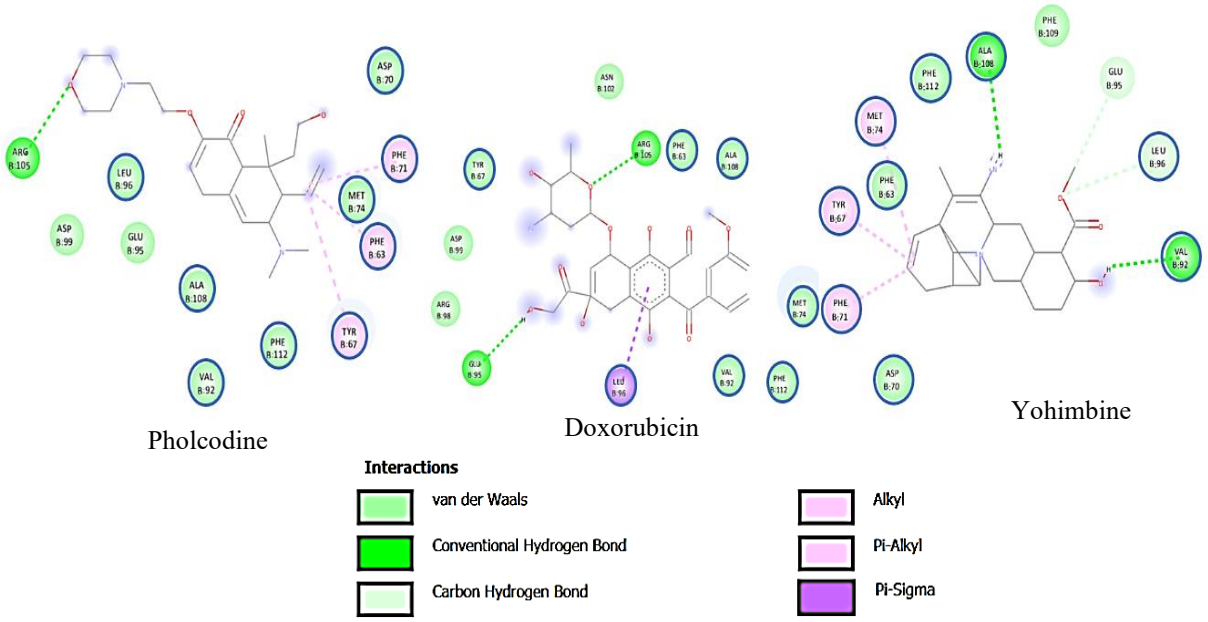

Figure 8 Interaction of Pholcodine and Yohimbine compounds compared with doxorubicin on 2W3L protein. Blue circles on amino acids indicate amino acid residues that are similar to the native ligand.

Pholcodine and polyneuridinealdehyde showed identical ΔG values of −8.3 kcal/mol. Both contain the same binding pocket yet exhibit variations in the quantity and type of amino acid residues. The percentage similarity of amino acid residue interactions with the native ligand can be identified, showing that Pholcodine exhibits a similarity of 45% and Polyneuridinealdehyde shows a similarity of 82%. Doxorubicin, serving as a positive control with a ΔG value of −8.7 kcal/mol, engages with the estrogen receptor via hydrogen bonds with Leu525's hydroxyl group and exhibits hydrophobic interactions with Trp383 and Ala350. Polyneuridinealdehyde contains similar amino acid residues with the native ligand and doxorubicin, including Trp383, Ala350, and Leu525, with non-covalent interactions. Pholcodine contains similar amino acid residues with the native ligand and doxorubicin, specifically Ala350 and Leu525, with non-covalent interactions and TRP383 with hydrophobic interactions. Despite doxorubicin exhibiting a lower ΔG value than Pholcodine and Polyneuridinealdehyde, the percentage similarity between the 2 compounds is greater. Both are anticipated to exhibit enhanced affinity and activity towards the estrogen receptor-α.

The ΔG value results for Bcl-2 are presented in **Table 4**. Two compounds exhibit ΔG values exceeding that of the positive control: −8.9 kcal/mol for Yohimbine and −7.0 kcal/mol for Pholcodine. Results amino acid residues involved in the interaction between ligand-estrogen receptors and ligand-Bcl-2 receptor can be seen in **Table 5**. **Figure 7** and **Figure 8** shows that both interact with all amino acid residues present in the native ligand, resulting in a similarity value of 100%. Furthermore, Yohimbine exhibits a hydrogen bond between the amino acid residue Val92 and the hydroxyl group, Ala108 and the amine group, as well as Leu96 and the O group. The existence of hydrogen bonds is anticipated to result in a lower ΔG value for Yohimbine compared to Pholcodine. The resemblance of amino acid residues interacting with the test compounds is anticipated to inhibit the Bcl-2 protein, consequently inducing cellular apoptosis. Yohimbine is an α2-adrenergic receptor antagonist that helps treat erectile dysfunction by acting as an aphrodisiac and stimulant. Yohimbine exhibits significant cytotoxic effect, with an IC_{50} value of 44μM against KB-ChR-8-5 oral cancer cells [34]. Pholcodine is an alkyl ether of morphine commonly utilised as an antitussive agent. The cytotoxicity assay of the oxycodone molecule, categorised with pholcodine, in hepatoma cells (Hep G2) indicates a considerable reduction in cell viability, diminished GSH levels, and lower total protein content in comparison to controls [35].

Polyneuridinealdehyde's possible anticancer properties have not been reported. Polyneuridinealdehyde is classified as an indole alkaloid chemical within the compound group. Indole alkaloids exhibit significant anti-tumor and anti-estrogenic properties against MCF-7 and MDA-MB-231 breast cancer cells [36]. According to the chemical class, indole alkaloids in kratom leaves have been shown by *in silico* to be able to inhibit estrogen receptor alpha and cause apoptosis by breaking the link between p53 and MDM2 and subsequently reactivating p53 activity [37]. Indole alkaloids have been shown to promote apoptosis in MCF-7 breast cancer cells by inhibiting the Bcl-2 protein [22].

Conclusions

Research finds that the alkaloid fraction of kratom leaves (*Mitragyna speciosa*) exhibits superior cytotoxic activity in T47D cells compared to kratom leaf extract samples. The alkaloid fraction was found 8 alkaloid compounds: 7-Hydroxymitragynine, Corynantheidine, Isorhynchophylline, Mitragynine, Pholcodine, Polyneuridinealdehyde, Rotundifolone, and Yohimbine. Moreover, Polyneuridinealdehyde exhibits the greatest potential *in silico* against estrogen receptors, while Yohimbine demonstrates significant efficacy against Bcl-2 receptors. To the best of our knowledge, this is the first report to investigate the apoptotic potential of polyneuridinealdehyde and yohimbine in breast cancer cells via *in silico* docking against estrogen receptors and Bcl-2 targets. Further research for the isolation of alkaloid compounds active against breast cancer and the mechanism of apoptosis is needed to realize the potential for active and safe cancer drugs.

Acknowledgments

The authors express their gratitude for the support provided by the *In Vitro* Laboratory Research Center 1, Faculty of Pharmacy, Airlangga University and the Pendidikan Magister Menuju Doktor untuk Sarjana Unggul (PMDSU) scholarship provided by the Ministry of Research, Technology, and Higher Education Indonesia. The research and higher education activities were financially supported by the Ministry of Research and Higher Education of Indonesia [PMDSU 2022 (NKI: 085/E5/PG.02.00.PT/2022) (NKT: 898/UN3.15/PT/2022)].

Declaration of Generative AI in Scientific Writing

The authors acknowledge the use of generative AI tools (e.g., QuillBot and ChatGPT by OpenAI) in the preparation of this manuscript, specifically for language editing and grammar correction. No content generation or data interpretation was performed by AI. The authors take full responsibility for the content and conclusions of this work

Credit Author Statement

Puja Adi Priatna: Conceptualization, Methodology, Supervision, Validation, Funding acquisition, and Writing –original draft

Siti Rahmah: Data curation, Formal analysis, Investigation, Validation, Visualization, Writing – original draft

Retno Widyowati: Methodology, Project administration, Resources, Supervision, Validation

Sukardiman: Idea concepts, Project administration, Resources, Supervision, Validation, Funding acquisition.

References

[1] H Sung, J Ferlay, RL Siegel, M Laversanne, I Soerjomataram, A Jemal and F Bray. Global cancer statistics 2020: GLOBOCAN estimates of incidence and mortality worldwide for 36 cancers in 185 countries. *CA: A Cancer Journal for Clinicians* 2021; **71(3)**, 209- 249.

[2] MT Chanu and AS Singh. Different types of Cancer treatment, its advancement, benefits, and side effects. *World Journal of Advanced Research and Reviews* 2024; **24(1)**, 571-580.

[3] U Anand, A Dey, AKS Chandel, R Sanyal, A Mishra, DK Pandey, VD Falco, A Upadhyay, R Kandimalla, A Chaudhary, JK Dhanjal, S Dewanjee, J Vallamkondu and JMPDL Lastra. Cancer chemotherapy and beyond: Current status, drug candidates, associated risks and progress in targeted therapeutics. *Genes & Diseases* 2023; **10(4)**, 1367-1401.

[4] D Conze, L Weiss, PS Regen, A Bhushan, D Weaver, P Johnson and M Rincon. Autocrine production of interleukin 6 causes multidrug resistance in breast cancer cells. *Cancer Res*earch 2001; **61(24)**, 8851-8858.

[5] ST Asma, U Acaroz, K Imre, A Morar, SR A Shah, SZ Hussain, D Arslan-Acaroz, H Demirbas, Z Hajrulai-Musliu, FR Istanbullugil, A Soleimanzadeh, D Morozov, K Zhu, V Herman, A Ayad, C Athanassiou and S Ince. Natural products/bioactive compounds as a source of anticancer drugs. *Cancers* 2022; **14(24)**, 6203.

[6] AL Harvey. Medicines from nature: Are natural products still relevant to drug discovery. *Trends in Pharmacological Sciences* 1999; **20(5)**, 196-198.

[7] M Ervina and Sukardiman. A review: Melia azedarach L. as a potent anticancer drug. *Pharmacognosy Reviews* 2018; **12(23)**, 94-102.

[8] NA Saidin, E Holmes, H Takayama and NJ Gooderham. The cellular toxicology of mitragynine, the dominant alkaloid of the narcotic-like herb, *Mitragyna speciosa* Korth. *Toxicology Research* 2015; **4(5)**, 1173-1183.

[9] L Flores-Bocanegra, HA Raja, TN Graf, M Augustinović, ED Wallace, S Hematian, JJ Kellogg, DA Todd, NBCech and NH Oberlies. The chemistry of kratom (*mitragyna speciosa*): Updated characterization data and methods to elucidate indole and oxindole alkaloids. *Journal of Natural Products* 2020; **83(7)**, 2165-2177.

[10] NA Saidin and NJ Gooderham. *In vitro* toxicology of extract of *Mitragyna speciosa* Korth, a malaysian phyto-pharmaceutical of abuse. *Toxicology* 2007; **240(3)**, 166-167.

[11] A Bayu, SI Rahmawati, F Karim, JA Panggabean, DP Nuswantari, DW Indriani, P Ahmadi, R Witular, NLPI Dharmayati and MY Putra. An *in vitro* examination of whether kratom extracts enhance the cytotoxicity of low-dose doxorubicin against A549 human lung cancer cells. *Molecules* 2024; **29(6)**, 1404.

[12] RS Wong. Apoptosis in cancer: From pathogenesis to treatment. *Journal of Experimental & Clinical Cancer Research* 2011; **30**, 87.

[13] A Susanty, D Dachriyanus, Y Yanwirasti, FS Wahyuni, P Amelia, F Frengk, I Ikhtiarudin, Y Hirasawa, T Kaneda and H Morita. Cytotoxic activity, and molecular docking of indole alkaloid voacangine and bisindole alkaloid vobtusine, vobtusine lactone from the indonesian plant: *voacanga foetida* (blume) rolfe. *Indonesian Journal of Pharmacy* 2021; **32(4)**, 442-443.

[14] TB Goh, KR Yian, MN Mordi and SM Mansor. Antioxidant value and antiproliferative efficacy of mitragynine and a silane reduced analogue. *Asian Pacific Journal of Cancer Prevention* 2014; **15(14)**, 5659-5665.

[15] G Domnic, NJ Chear, A Rahman, S Ramanathan, K Lo, D Singh and N Mohana-Kumaran. Combinations of indole based alkaloids from *Mitragyna speciosa* (Kratom) and cisplatin inhibit cell proliferation and migration of nasopharyngeal carcinoma cell lines. *Journal Ethnopharmacology* 2021; **279**, 114391.

[16] PA Priatna, R Widyowati and Sukardiman. Cytotoxic potential of *mitragyna speciosa* as anticancer - a review. *Pharmacognosy Journal* 2024; **16(6)**, 1418-1423.

[17] K Liu, P Liu, R Liu and X Wu. Dual AO/EB staining to detect apoptosis in osteosarcoma cells compared with flow cytometry. *Medical Science Monitor Basic Research* 2015; **9(21)**, 15-20.

[18] M Pan, Q Lei, N Zang and H Zhang. A strategy based on GC-MS/MS, UPLC-MS/MS and virtual molecular docking for analysis and prediction of bioactive compounds in *Eucalyptus globulus* Leaves. *International Journal of Molecular Sciences* 2019; **20(16)**, 3875.

[19] MS Zubair, S Maulana, A Widodo, R Pitopang, M Arba and M Hariono. GC-MS, LC-MS/MS, docking and molecular dynamics approaches to identify potential SARS-CoV-2 3-chymotrypsin-like protease inhibitors from *Zingiber officinale* roscoe. *Molecules* 2021; **26(17)**, 5230.

[20] RR Pratama, I Sholikhah, Sukardiman, RK Sahu and R Widyowati. Phytochemical compounds identification from 70% ethanol extract of *arcangelesia flava* (L.) merr stems using LC-MS/MS and *in silico* molecular docking approach as inhibitor interleukin-1β. *Pharmacognosy Journal* 2023; **15(4)**, 528-534.

[21] PA Priatna, S Rahmah, R Widyowati and Sukardiman. Identification of LC-MS/MS and docking analysis of topoisomerase IIα inhibition from kratom leaves (*mitragyna speciosa*) as potential anticancer agents. *International Journal of Applied Pharmaceutics* 2025; **17(1)**, 119-125.

[22] A Sharma, SH Kamble, F Leon, NJY Chear, TI King, EC Berthold, S Ramanathan, CR McCurdy and BA Avery. Simultaneous quantification of ten key Kratom alkaloids in *Mitragyna speciosa* leaf extracts and commercial products by ultra-performance liquid chromatography−tandem mass spectrometry. *Drug Testing and Analysis* 2019; **11(8)**, 1162-1171.

[23] FS Wahyuni, S Febria and D Arisanty. Apoptosis induction of cervical carcinoma hela cells line by dichloromethane fraction of the rinds of garcinia cowa roxb. *Pharmacognosy Journal* 2017; **9(4)**, 475-478.

[24] N Sreevidya and S Mehrotra. Spectrophotometric method for estimation of alkaloids precipitable with dragendorff's reagent in plant materials. *Journal of AOAC International* 2003; **86(6)**, 1124-1127.

[25] B Thanuja, R Parimalavalli, S Vijayanan, RM Alharbi, N Abdel-Raouf, IBM. Ibraheem, EN Sholkamy, K Durairaj and KM Hadish. Anticancer and cytotoxicity activity of native and modified black rice flour on colon cancer cell lines. *Evidence-Based Complementary and Alternative Medicine* 2022; **2022(1)**, 8575026.

[26] R Lifiani, U Harahap, PAZ Hasibuan and D Satria. Anticancer effect of african leaves (*Vernonia amygdalina* del.) to T47D cell resistant. *Asian Journal of Pharmaceutical and Clinical Research* 2018; **11(13)**, 4-7.

[27] R Qin, F You, Q Zhao, X Xie, C Peng, G Zhan and B Han. Naturally derived indole alkaloids targeting regulated cell death (RCD) for cancer therapy: from molecular mechanisms to potential therapeutic targets. *Journal of Hematology & Oncology* 2022; **15**, 133.

[28] Z Hassan, M Muzaimi, V Navaratnam, NHM Yusoff, FW Suhaimi, R Vadivelu, BK Vicknasingam, D Amato, SV Horsten, NIW Ismail, N Jayabalan, AI Hazim, SM Mansor and CP Muller. From Kratom to mitragynine and its derivatives: physiological and behavioural effects related to use, abuse, and addiction. *Neuroscience & Biobehavioral Reviews* 2013; **37(2)**, 138-151.

[29] FZ Karadayi, M Yaman, MM Kisla, AG Keskus, O Konu and Z Ates-Alagoz. Design, synthesis and anticancer/antiestrogenic activities of novel indole-benzimidazoles. *Bioorganic Chemistry* 2020; **100**, 103929.

[30] S Zaman, R Wang and V Gandhi. Targeting the apoptosis pathway in hematologic malignancies. *Leukemioa & Lymphoma* 2014; **55(9)**, 1980-1992.

[31] J Lopez and SWG Tait. Mitochondrial apoptosis: Killing cancer using the enemy within. *British Journal of Cancer volume* 2015; **112(6)**, 957-692.

[32] JL Nelsen, J Lapoint, MJ Hodgman and KM Aldous. Seizure and coma following kratom (*Mitragynina speciosa* Korth) exposure. *Jounal of Medical Toxicology* 2010; **6(4)**, 424-426.

[33] AK Shiau, D Barstad, PM Loria, L Cheng, PJ Kushner, DA Agard and GL Greene. The structural basis of estrogen receptor/coactivator recognition and the antagonism of this interaction by tamoxifen. *Cell* 1998; **95(7)**, 927-937.

[34] NR Jabir, MS Khan, NO Alafaleq, H Naz and BA Ahmed. Anticancer potential of yohimbine in drug-resistant oral cancer KB-ChR-8-5 cells. *Molecular Biology Reports* 2022; **49(10)**, 9565-9573.

[35] M Jairaj, DG Watson, MH Grant and GG Skellern. The toxicity of opiates and their metabolites in HepG2 cells. *Chemico-Biological Interactions* 2003; **146(2)**, 121-129.

[36] FZ Karadayi, M Yaman, MM Kisla, AG Keskus, O Konu and Z Ates-Alagoz. Design, synthesis and anticancer/antiestrogenic activities of novel indole-benzimidazoles. *Bioorganic Chemistry* 2020; **100**, 103929.

[37] PA Priatna, RR Pratama, R Widyowati and Sukardiman. Molecular docking estrogen receptor alpha antagonist and P53-MDM2 inhibitor, ADMET prediction of alkaloid compound from *mitragyna speciosa* for breast cancer therapy. *Pharmacognosy Journal* 2022; **14(6)**, 912-916.

[38] R Veeramohan, KA Azizan, WM Aizat, Metabolomics data of *Mitragyna speciosa* leaf using LC-ESI-TOF-MS. *Data Brief* 2018; **18**, 1212-1216.

[39] B Avula, S Sagi and YH Wang. Identification and characterization of indole and oxindole alkaloids from leaves of *Mitragyna speciosa* Korth using liquid chromatography-accurate QToF mass spectrometry. *Journal of AOAC International* 2015; **98(1)**, 13-21.